Available online at www.sciencedirect.com

jmr&t Journal of Materials Research and Technology

journal homepage: www.elsevier.com/locate/jmrt

Original Article

Fatigue strength assessment of riveted railway bridge details based on regression analyses combined with probabilistic models

José Correia [a,*], *António Mourão* [a], *Haohui Xin* [b,**], *Abílio De Jesus* [c], *Túlio Bittencourt* [d], *Rui Calçada* [a], *Filippo Berto* [f]

[a] *CONSTRUCT, Faculty of Engineering, University of Porto, 4200-465 Porto, Portugal*
[b] *Department of Civil Engineering, School of Human Settlements and Civil Engineering, Xi'an Jiaotong University, Xi'an, China*
[c] *INEGI, Faculty of Engineering, University of Porto, 4200-465 Porto, Portugal*
[d] *Polytechnic School, University of São Paulo, 05508-010 São Paulo, Brazil*
[f] *Department of Mechanical and Industrial Engineering, Norwegian University of Science and Technology (NTNU), Norway*

ARTICLE INFO

Article history:
Received 5 August 2022
Accepted 27 January 2023
Available online 1 February 2023

Keywords:
Riveted joints
Fatigue strength
S–N curve
Statistical model
Probability models

ABSTRACT

With the increasing attention on structural reliability and integrity, the probabilistic fatigue behaviour of riveted joints is drawn more attention, more specifically in the influence that this may have on the fatigue damage accumulation evaluation of structural components. For that, in this paper, the parameters of S–N curves for two riveted joints were obtained using the least-squares regression (LR) and the orthogonal regression (OR) methods, respectively. The results showed that the fitted slope B from the OR method is larger than the one from the LR method of all specimens. The probabilistic fatigue life of the riveted joints is obtained by Castillo & Fernández-Canteli (CFC) method and stochastic analysis using Latin hypercube sampling strategies. Among six different probabilistic functions, the stochastic analysis with the Gumbel distribution contributed to the largest fatigue strength with 95% and 99% confidence levels while the stochastic analysis with the Weibull distribution led to the smallest fatigue strength with 95% and 99% confidence levels. The effects of regression methods on the probabilistic fatigue life are not obvious, however, for the levels of stress range of the high-cycle regime, the fatigue life is substantially different when the comparison is made between the curves obtained by different approaches, which will have implications in the assessment of the fatigue damage accumulation of structural joints operating in this fatigue regimes. The fatigue strength with 95% and 99% confidence levels obtained using constant exponent are larger than when employing the varied exponent. The probabilistic fatigue life with stochastic analysis using constant exponent is closer to the CFC model than by using varied constant.

* Corresponding author.
** Corresponding author.
E-mail addresses: jacorreia@fe.up.pt (J. Correia), amourao@fe.up.pt (A. Mourão), xinhaohui@xjtu.edu.cn (H. Xin), ajesus@fe.up.pt (A. De Jesus), tbitten@usp.br (T. Bittencourt), ruiabc@fe.up.pt (R. Calçada), filippo.berto@ntnu.no (F. Berto).
https://doi.org/10.1016/j.jmrt.2023.01.193

1. Introduction

After a long period of service, fatigue crack initiation [1,2] and propagation [3,4] are the main concerns for the old riveted steel bridges [5–11], especially the load and amount of vehicles increased a lot compared with the previous design specification. The fatigue strength of riveted joints plays an important role during the fatigue performance evaluation of such type of steel bridges.

Ensuring the safety of riveted joints against fatigue consists of developing two research themes, one related to the estimation of the current damage in the structure and the other related to the estimation of the remaining life. The fatigue behaviour of riveted joints was investigated through both experiments and numerical analysis [12–17] for better prediction of the fatigue life of such old riveted steel bridges.

The fatigue performance prediction of old riveted joints could be very complex. In terms of the design specification of EC3 [18], Class 71 S–N curve is recommended by Kühn et al. [19] to assess the fatigue behaviour of riveted joints. But further investigations for more detailed categorization of riveted joints are recommended by several works [20–32] because Class 71 category of EC3 [18] generally contributes to conservative fatigue life predictions.

With the increasing attention on structural reliability and integrity, the probabilistic fatigue behaviour of riveted joints has called more attention. The fatigue life considering multiple uncertainty source effects are essential for the determination of the riveted details. Correia [33,34] proposed a probabilistic S–N field based on Castillo & Fernández-Canteli (CFC) model [35] using the Weibull distribution function and UniGrow approach for the notched details. Reliable Wöhler curves based on the Stüssi model and the Weibull distribution function were suggested by Caiza et al. [15] to strength the modelling of structural details. Zhu et al. [36] investigated the fatigue life distribution of notched specimens based on the Weibull model and critical distance theory. Besides, the stochastic analysis allows us to obtain the probabilistic fatigue behaviour of riveted joints based on meta modelling [37]. A comparison between Castillo & Fernández-Canteli (CFC) method [35] and stochastic meta modelling is expected to provide an initial impression for the analysis of probabilistic fatigue life using different methods.

In this paper, the parameters of S–N curves for two riveted joints made of S235JR structural steel ("single line double shear riveted" – SLDSR and "double line double shear riveted" – DLDSR) were obtained using both the least-squares regression and the orthogonal regression methods, where the root-mean square errors (RMSE) are calculated. The probabilistic fatigue life fields were firstly obtained based on Castillo & Fernández-Canteli (CFC) method [35] using experimental data. After that, the stochastic analysis using Latin hypercube sampling strategies and different probability functions were conducted to obtain probabilistic fatigue life fields. The probabilistic fatigue behaviour obtained by these two methods were compared and discussed.

Nomenclature

A	Regression parameter (log(Δσ)–log(N) scale)
Ave	Average value
B	Regression parameter (negative inverse slope, m); Threshold parameter for the lifetime (CFC method)
C	Intercept of N-axis by S–N curve (Material constant); Threshold parameter for stress range (CFC method)
CFC	Castillo & Fernández-Canteli model
DLDSR	double line double shear riveted
Fmax	Maximum force
Fmin	Minimum force
LR	Least-squares regression
m	Negative inverse slope of S–N curve (material constant)
N	Number of cycles to failure
Nf	Fatigue life
OR	Orthogonal regression
PDF	probability density function
Pf	Failure probability
R	Load ratio
Std	Standard deviation
SLDSR	Single line double shear riveted
V	Normalized variable (CFC method)
Δ F	Force range
Δ σ	Stress range
Δ σtotal	Stress range of the gross cross-section
Δσnet	Stress range of the net cross-section
β	Shape parameter of Weibull model
δ	Scale parameter
λ	Threshold parameter for normalized variable V

2. Experimental results

The riveted joints of the Trezói Bridge were made of St37 steel grade, close to the current S235JR structural steel grade, according to the European standards. Consequently, the specimens of the riveted joints under consideration – "single line double shear riveted" (SLDSR) and (double line double shear riveted" (DLDSR) – were manufactured using two different materials, namely the S235JR structural steel for the plates, beams, and angles, and the rivet material. According to Silva et al. [38], the microstructure of the riveted material reveals to have a smaller grain size when compared with the current S235JR structural steel.

In this section, the microstructural analysis and mechanical properties of the S235JR structural steel are presented. Besides, the fatigue resistance results of the SLDSR and DLDSR riveted joints are detailed, where the mean S–N curves by applying linear regression methods (Least-squares Regression – LR, Orthogonal Regression – OR) are estimated. From the application of the linear regression methods to the fatigue resistance results of the riveted joints under consideration, the root-mean-square errors (RMSE) are calculated.

Table 1 – Chemical composition of the S235JR structural steel used in the riveted joints (Wt., %).

Steel Grade	C%	Mn%	Si%	P%	S%	N%	Mo%	B%
	max	max	max	max	max	max	max	max
S235JR	0.190	1.500	0.030	0.045	0.045	0.014	–	–

Table 2 – Tensile properties of the S235JR structural steel used in the riveted joints.

Steel Grade	R_p	R_m	Elongation@ fracture
	[MPa]	[MPa]	%
S235JR	235	360–510	26

2.1. *Microstructural analysis and mechanical properties*

Tables 1 and 2 show the chemical composition and tensile properties for the S235JR structural steel used in the SLDSR and DLDSR riveted joints under consideration, respectively.

Fig. 1 plots the observed microstructure of the S235JR structural steel by using optical microscopy. In this study, magnifications of 200 ×, 500 ×, and 1000 × were considered. A global analysis of the micrograph of the S235JR structural steel allowed to observe a typical microstructure of a carbon structural steel, namely an equilibrium microstructure of perlite (dark zone) and ferrite (white zone) is observed [38].

2.2. *Fatigue resistance results of riveted joints*

A total of 19 specimens [38], including 10 SLDSR specimens and 9 DLDSR specimens, were tested under fatigue loading.

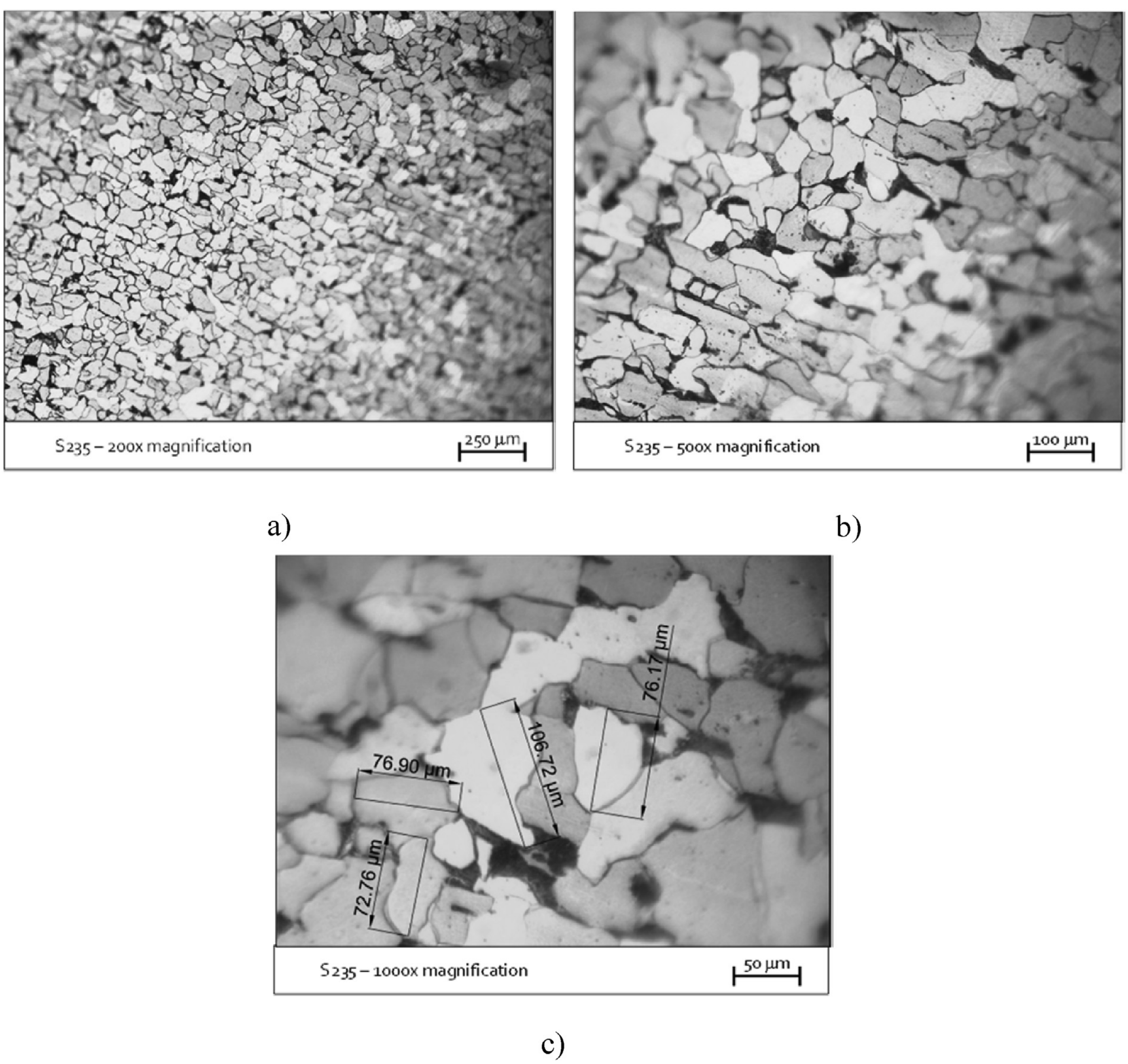

Fig. 1 – Microstructure of S235JR structural steel: a) magnification of 200; b) magnification of 500; c) magnification of 1000.

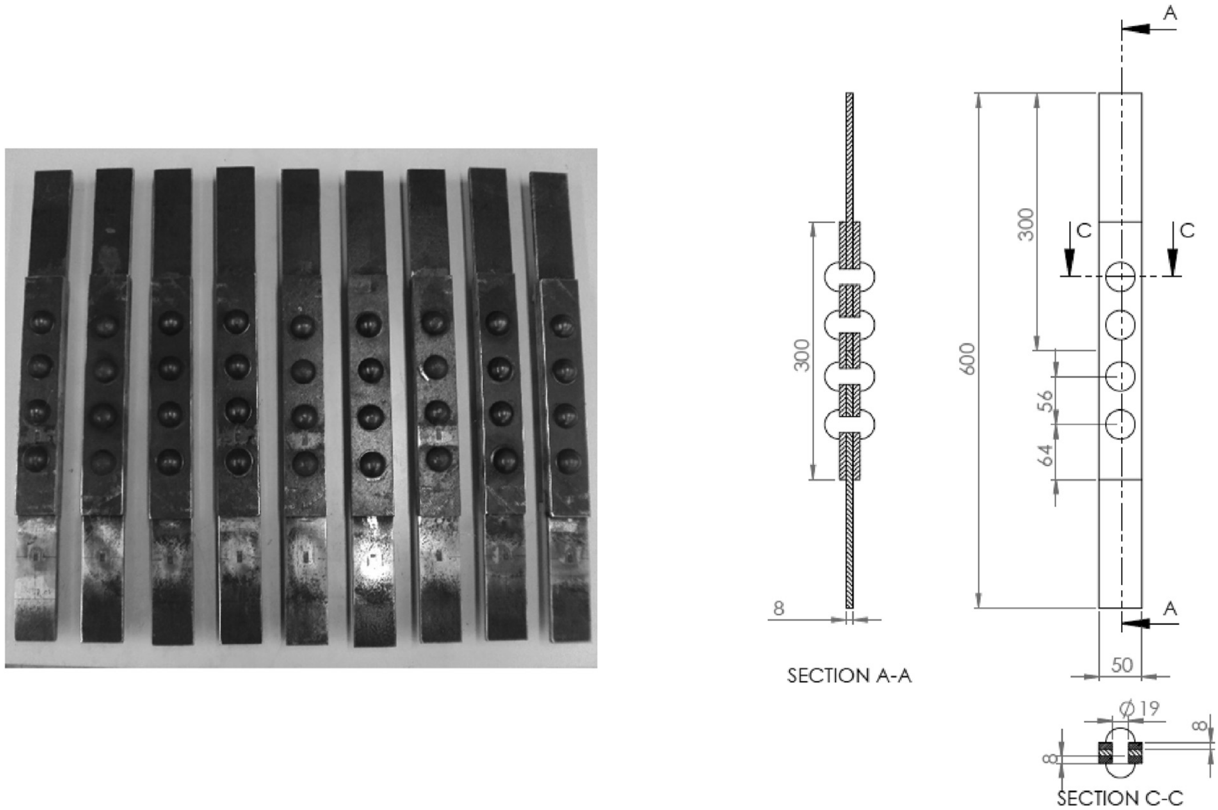

Fig. 2 – Single line double shear riveted (SLDSR) specimens [38].

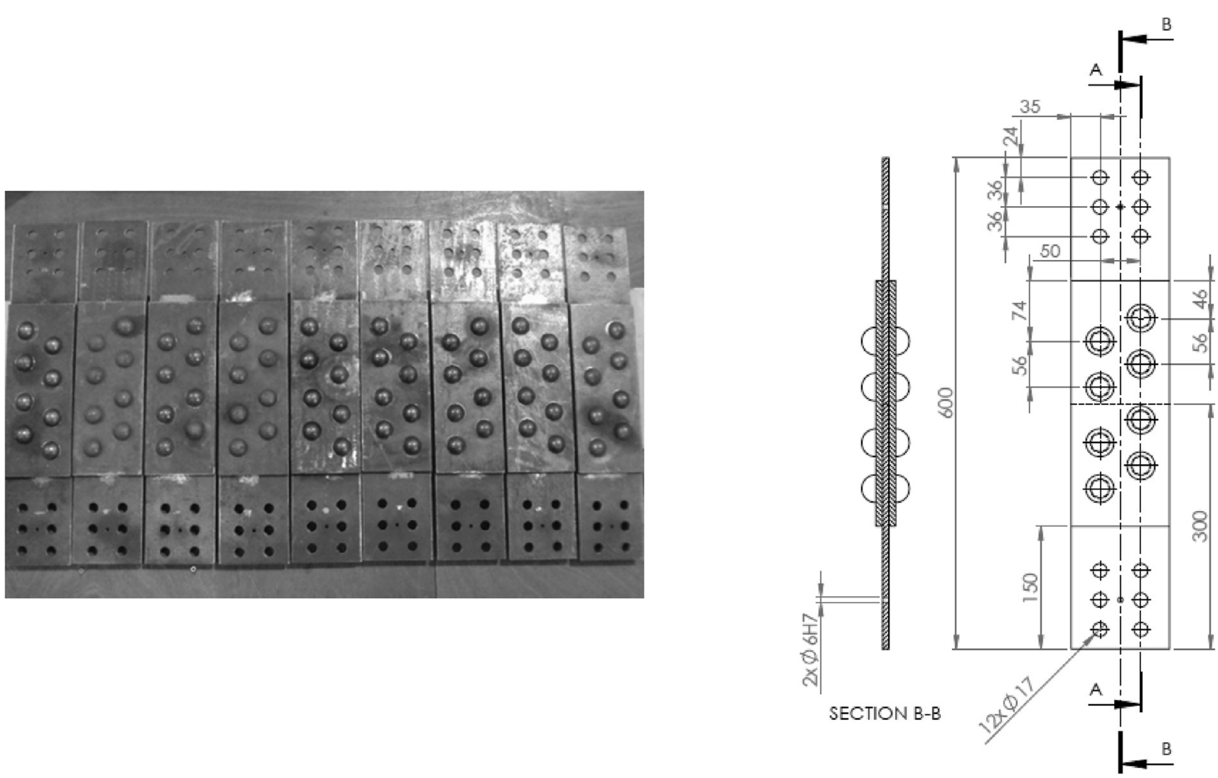

Fig. 3 – Double line double shear riveted (DLDSR) specimens [38].

Table 3 – Fatigue test results of SLDSR specimens [38].

Specimens	Load R-ratio	F_{max} [kN]	F_{min} [kN]	ΔF [kN]	$\Delta\sigma_{total}$ [MPa]	$\Delta\sigma_{net}$ [MPa]	N_f
SLDSR -01[a]	0.01	50.00	0.50	49.5	122.6	198.0	391735[a]
SLDSR -02	0.01	95.95	0.96	94.99	232.8	375.7	28764
SLDSR -03	0.01	95.00	0.95	94.05	234.9	379.6	18631
SLDSR -04	0.01	80.00	0.80	79.20	194.8	314.2	361858
SLDSR -05	0.01	65.00	0.65	64.35	160.2	258.9	807561
SLDSR -06	0.01	80.00	0.80	79.20	198.1	320.2	47843
SLDSR -07	0.01	60.00	0.60	59.40	147.7	238.3	1130000
SLDSR -08	0.01	80.00	0.80	79.20	196.7	317.7	127102
SLDSR -09	0.01	70.00	0.70	69.30	171.9	277.8	868598
SLDSR -10	0.01	95.95	0.96	94.99	235.3	379.9	77904

[a] Run-out (excluded during fitting).

Table 4 – Fatigue test results of DLDSR specimens [38].

Specimens	R	F_{max} [kN]	F_{min} [kN]	ΔF [kN]	$\Delta\sigma_{total}$ [MPa]	$\Delta\sigma_{net}$ [MPa]	N_f
DLDSR -01	0.10	160.00	16	144	148.7	176.9	660121
DLDSR -02	0.10	180.00	18	162	167.1	199.3	455794
DLDSR -03	0.10	100.00	10	90	92.8	110.4	3125148
DLDSR -04	0.10	120.00	12	108	112.4	133.9	1633734
DLDSR -05	0.10	120.00	12	108	112.4	133.9	1146928
DLDSR -06	0.10	200.00	20	180	187.1	222.7	208727
DLDSR -07	0.10	120.00	12	108	112.3	133.7	1633734
DLDSR -08	0.10	180.00	18	162	167.2	198.8	309294
DLDSR -09	0.10	160.00	16	144	148.6	176.6	662938

The photos and geometry of SLDSR and DLDSR specimens are shown in Figs. 2 and 3, respectively.

The SLDSR specimens were tested in an INSTRON 8801 servo-hydraulic machine (capacity of 100 kN) using a load R-ratio of 0.01. The DLDSR specimens were tested by using an MTS servo-hydraulic machine (capacity of 250 kN), under a load R-ratio of 0.1.

The fatigue test results of SLDSR and DLDSR specimens are listed in Tables 3 and 4, including the load ratio R, maximum force F_{max} and minimum force F_{min}, the stress range of the net cross-section $\Delta\sigma_{net}$, and fatigue life N_f. More details about experimental tests can be found in Silva et al. [38].

According to design codes, the fatigue strength curves, called S–N or Wöhler curves, of materials and/or structural details are given by:

$$\Delta\sigma^m N = C \quad (1)$$

where: $\Delta\sigma$ is the stress range; N is the number of cycles to failure; C and m are material constants. Alternatively, the S–N curve [39], expressed in Eq. (2), is used to describe the relationship between stress range, $\Delta\sigma$, and fatigue life, N:

$$\Delta\sigma = AN^B \quad (2)$$

or

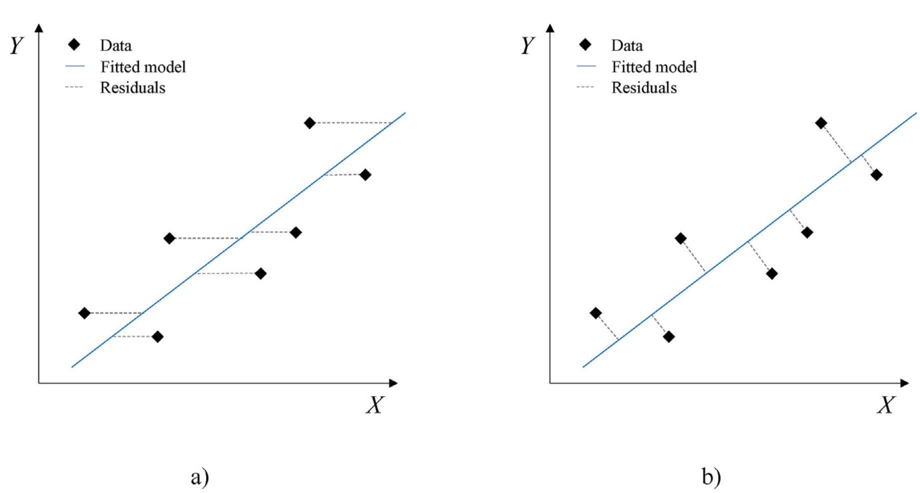

Fig. 4 – Linear regression methods: a) least-squares regression (LR); b) orthogonal regression (OR).

Table 5 – The fitted material parameters of the S–N curve.

Specimens	Least-squares Regression (LR)					Orthogonal Regression (OR)				
	A		B		RMSE (LogN)	A		B		RMSE (LogN)
	Ave.	Std.	Ave.	Std.		Ave.	Std.	Ave.	Std.	
SLDSR	25.9414	3.6447	8.3040	1.4591	0.2699	30.3695	4.0109	10.0774	1.6057	0.2971
DLDSR	13.7938	0.6148	3.5772	0.2783	0.0721	14.1049	0.6260	3.7181	0.2834	0.0734
SLDSR + DLDSR	12.8460	1.1997	3.1008	0.5088	0.3421	15.7704	1.4059	4.3442	0.5962	0.4009

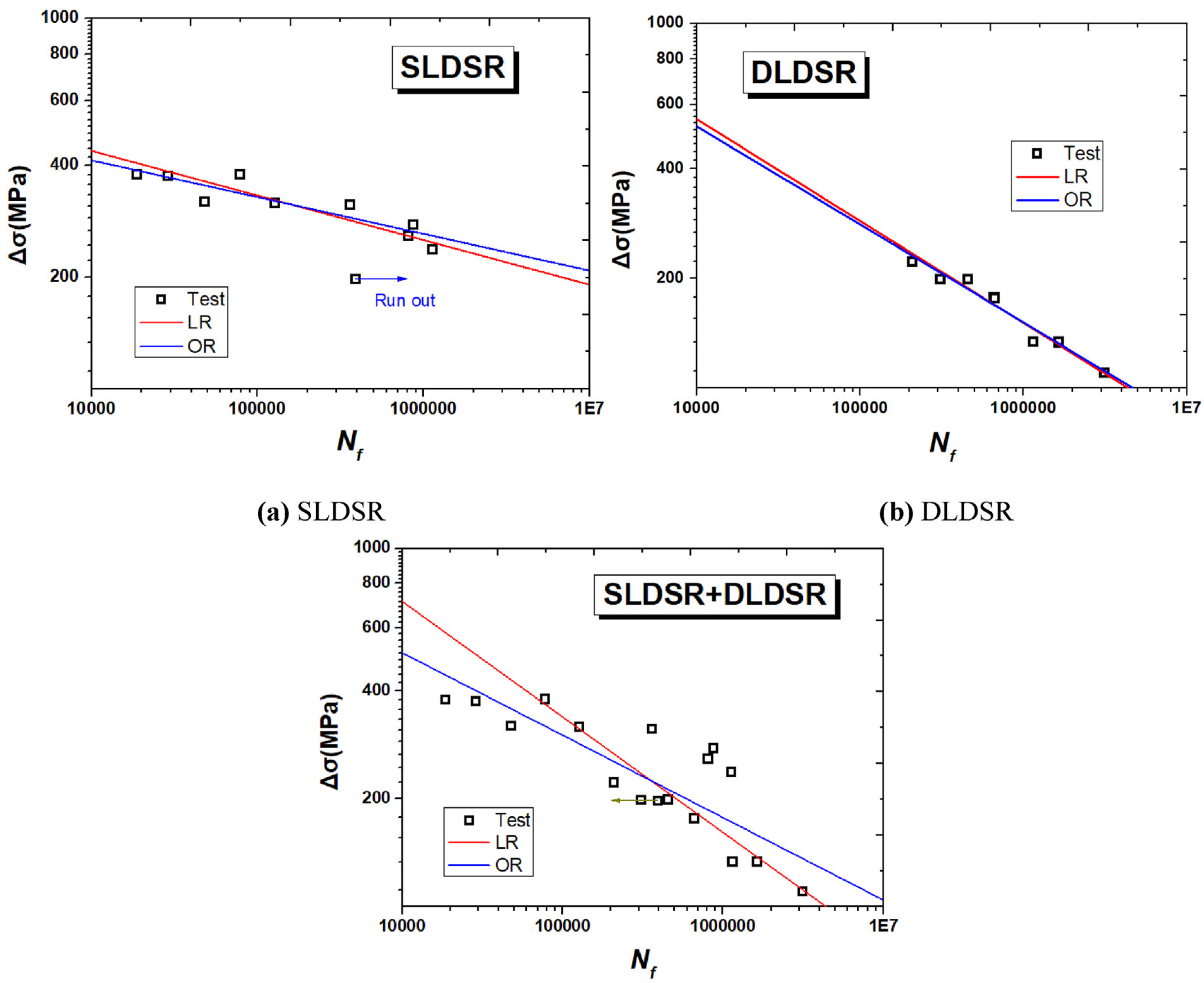

(a) SLDSR (b) DLDSR

(c) SLDSR+ DLDSR

Fig. 5 – Comparisons between fitted S–N curves and experimental data (Stress range, $\Delta\sigma$, vs. number of cycles, N_f).

Table 6 – Material parameters of CFC models.

Specimens	B	C	N_0	$\Delta\sigma_0$	λ	δ	β
SLDSR	9.2	5.3	1.58×10^9	2.00×10^5	0.00	1.26	3.10
DLDSR	0.0	1.2	1.0	15.8	43.73	9.12	15.25
SLDSR + DLDSR	0.0	1.0	1.0	10.0	46.33	11.25	2.80

$$\log(N) = A - B\log(\Delta\sigma) \tag{3}$$

where: A and B are regression parameters estimated by applying linear regression methods. These A and B regression parameters can be related to the C and m material and/or structural detail parameters of the design codes curves as follows:

$$C = 10^{A} \tag{4}$$

$$m = -B \tag{5}$$

The material parameters A and B are fitted by the least-squares regression (LR) [40] and the orthogonal regression (OR) [41] using the linear Equation (3). The LR method (Fig. 4a) aims to approximate the solution by minimizing the sum of the squares of the residuals between every single data point and the regression line. The error in the independent variable is negligible of the LR method. The sum of the squares of the LR method is to be calculated in Equation (6). While the OR method (Fig. 4b) assumes that both independent and dependent variables may be subject to error and the sum of squares is to be calculated in Equation (7).

$$E_{LR} = \sum_{i=1}^{n}\left(y_i - \hat{y}_i\right)^2 = \sum_{i=1}^{n}\left(y_i - B_{LR}x_i - A_{LR}\right)^2 \tag{6}$$

$$E_{OR} = \sum_{i=1}^{n}\frac{\left(y_i - B_{OR}x_i - A_{OR}\right)^2}{{B_{OR}}^2 + 1} \tag{7}$$

In Table 5, the fitted material parameters are summarized. The comparisons between the experimental observations and fitted S–N curves are shown in Fig. 5. The results showed that the fitted slope B from the OR method is larger than the result from the LR method for both specimen series. In the relatively lower-stress range (medium- and high-cycle regimes), the parameters from the OR method predicted the longer fatigue lives than that from the LR method, detailed as $0 < \Delta\sigma \leq 305$ MPa for SLDSR specimen, $0 < \Delta\sigma \leq 160$ MPa for DLDSR

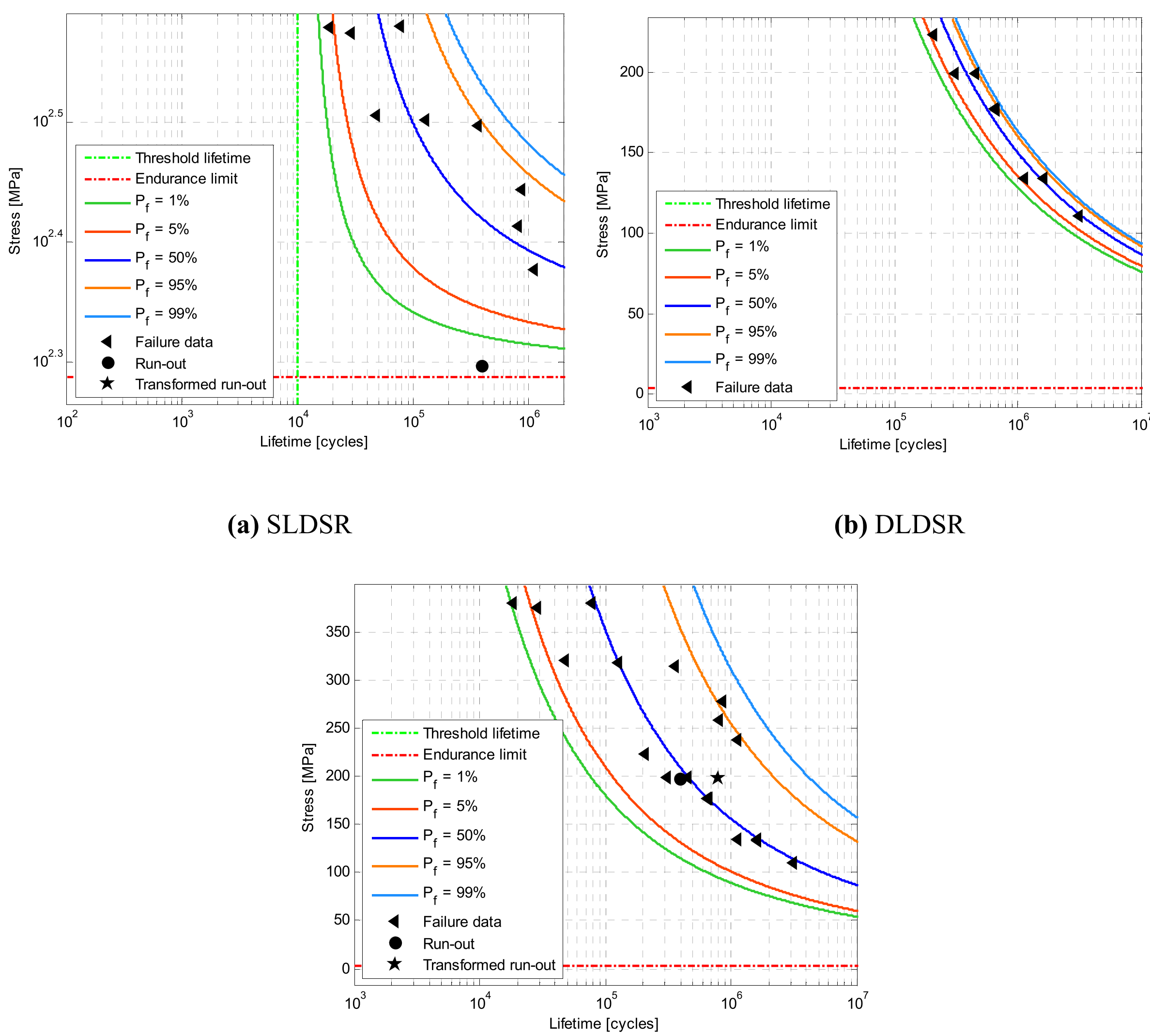

(a) SLDSR (b) DLDSR

(c) SLDSR+ DLDSR

Fig. 6 – P–S–N fields for different riveted details test data.

specimen, and $0 < \Delta\sigma \leq 223$ MPa for "SLDSR + DLDSR" results. In the upper-stress range (low- and medium-cycle regimes), the parameters from the OR method predicted the shorter fatigue lives than that from the LR method, detailed as $\Delta\sigma > 305$ MPa for SLDSR specimen, $\Delta\sigma > 160$ MPa for DLDSR specimen, and $\Delta\sigma > 223$ MPa for "SLDSR + DLDSR" results.

The standard derivation S_A for material parameter A and S_B for material parameter B is also calculated by definition of $y = \log(N)$ and $x = \log(\Delta\sigma)$ using Equations 8–10. The values of S_A and S_B are listed in Table 5. It is noted that the standard derivation obtained from the OR method is slightly larger than that from the LR method.

$$S_A = S\left(\frac{1}{n} + \frac{\bar{x}^2}{\sum x_i^2 - \left(\sum x_i\right)^2/n}\right)^{1/2} \tag{8}$$

$$S_B = S\left(\frac{1}{\sum x_i^2 - \left(\sum x_i\right)^2/n}\right)^{1/2} \tag{9}$$

$$S = \left(\frac{\sum (y_i - \bar{y}_i)^2}{n-2}\right)^{1/2} \tag{10}$$

Table 7 – Parameters estimated of each probability density function under consideration.

Name	Probability density function			SLDSR	DLDSR	SLDSR + DLDSR
Gaussian distribution	$f_X(x) = \frac{1}{\sigma\sqrt{2\pi}} e^{-\frac{(x-\mu)^2}{2\sigma^2}}$	LR	μ_A	25.94	13.79	12.85
			σ_A	3.64	0.61	1.20
			μ_B	8.30	3.58	3.10
			σ_B	1.46	0.28	0.51
		OR	μ_A	30.37	14.10	15.77
			σ_A	4.01	0.63	1.41
			μ_B	10.08	3.72	4.34
			σ_B	1.61	0.28	0.59
Lognormal distribution	$f_X(x) = \frac{1}{\sqrt{2\pi}\zeta x} exp\left(-\frac{(\ln x - \lambda)^2}{2\zeta^2}\right)$	LR	λ_A	3.24	2.62	2.55
			ζ_A	1.40	0.04	0.09
			λ_B	2.10	1.27	1.12
			ζ_B	1.74	0.08	0.16
		OR	λ_A	3.41	2.05	2.75
			ζ_A	0.13	0.04	0.09
			λ_B	2.30	1.31	1.46
			ζ_B	1.58	0.08	0.14
Weibull distribution	$f_X(x) = \begin{cases} \frac{\beta}{\alpha}\left(\frac{x}{\alpha}\right)^{\beta-1} e^{-(x/\alpha)^\beta}, \text{if } x \geq 0 \\ 0, x<0 \end{cases}$	LR	α_A	27.50	14.07	13.36
			β_A	8.48	28.07	13.06
			α_B	8.90	3.70	3.31
			β_B	6.67	15.80	7.18
		OR	α_A	32.06	14.38	16.38
			β_A	9.06	28.19	13.71
			α_B	10.74	3.84	4.60
			β_B	7.41	1.61	8.70
Gamma distribution	$f_X(x) = \frac{\lambda^k}{\Gamma(k)} x^{k-1} e^{-\lambda x}$	LR	λ_A	1.95	36.49	8.93
			k_A	50.67	503.40	114.70
			λ_B	3.90	46.19	11.98
			k_B	32.39	165.20	37.14
		OR	λ_A	1.89	35.99	7.98
			k_A	57.33	507.70	125.80
			λ_B	3.91	46.29	12.22
			k_B	39.40	172.10	53.09
Logistic distribution	$f_X(x) = \frac{e^{-\frac{x-\mu}{s}}}{s\left(1+e^{-\frac{x-\mu}{s}}\right)^2}$	LR	μ_A	25.94	13.79	12.85
			s_A	2.01	0.34	0.66
			μ_B	8.30	3.58	3.10
			s_B	0.80	0.28	0.28
		OR	μ_A	30.37	14.10	15.77
			s_A	2.21	0.35	0.78
			μ_B	10.08	3.72	4.34
			s_B	0.89	0.16	0.33
Gumbel distribution	$f_X(x) = \frac{1}{\beta} e^{-\frac{x-\mu}{\beta} - e^{-\frac{x-\mu}{\beta}}}$	LR	μ_A	24.30	13.52	12.31
			β_A	2.84	0.48	0.94
			μ_B	7.65	3.45	2.87
			β_B	1.14	0.22	0.40
		OR	μ_A	28.56	13.82	15.14
			β_A	3.13	0.49	1.09
			μ_B	9.36	3.59	4.08
			β_B	1.25	0.22	0.46

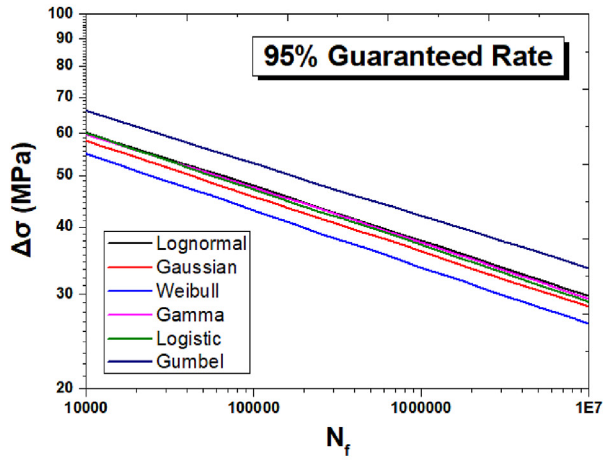

(a) 95% Confidence level

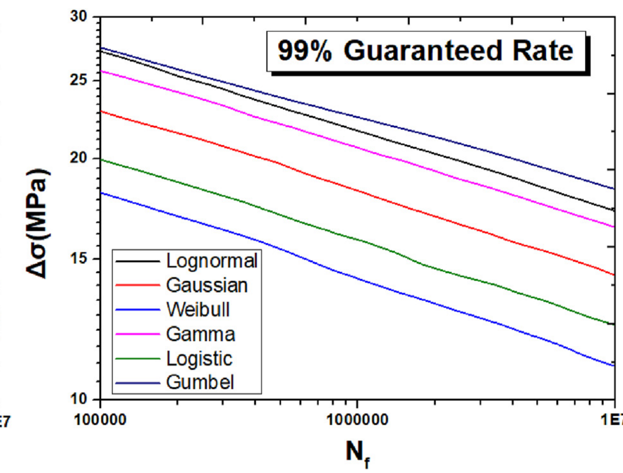

(b) 99% Confidence level

Fig. 7 – S–N curves comparison with 95% and 99% Confidence levels obtained with different probabilistic functions using the standard derivation of the least-squares regression.

Table 8 – The fitted material parameters of the S–N curve with different probabilistic functions using the standard derivation of the least-squares regression.

Functions		SLDSR		DLDSR		SLDSR + DLDSR	
		A	B	A	B	A	B
Lognormal	95% confidence level	21.6588	10.1485	13.0252	3.9188	11.4617	3.7717
	99% confidence level	20.6714	11.3244	12.7505	4.0869	10.9360	4.0992
Gaussian	95% confidence level	21.0050	9.8791	12.9885	3.9028	11.2503	3.6693
	99% confidence level	19.1775	10.5856	12.6515	4.0240	10.6007	3.8999
Weibull	95% confidence level	20.3990	9.6169	12.8141	3.8143	10.9911	3.5732
	99% confidence level	17.1774	9.9466	12.1291	3.8301	9.7515	3.6539
Gamma	95% confidence level	21.4503	10.0389	13.0264	3.9092	11.4144	3.7368
	99% confidence level	19.9581	11.0811	12.7358	4.0643	10.8745	4.0640
Logistic	95% confidence level	21.1522	9.9110	12.9840	3.8874	11.2683	3.6684
	99% confidence level	18.4872	10.5598	12.6292	4.0711	10.4211	3.9203
Gumbel	95% confidence level	22.5159	10.3895	13.2417	4.0001	11.7341	3.8388
	99% confidence level	22.2392	12.1443	13.1700	4.3383	11.5937	4.4508

Table 9 – The fitted material parameters of the S–N curve with different probabilistic functions using the standard derivation of the orthogonal regression.

Functions		SLDSR		DLDSR		SLDSR + DLDSR	
		A	B	A	B	A	B
Lognormal	95% confidence level	25.7537	12.1197	13.3356	4.0610	14.0943	5.0960
	99% confidence level	24.3500	13.3060	13.0626	4.2466	13.5625	5.5246
Gaussian	95% confidence level	24.9809	11.8470	13.2991	4.0452	13.9302	5.0353
	99% confidence level	22.7827	12.5331	12.9596	4.1832	13.1197	5.2771
Weibull	95% confidence level	24.2640	11.4933	13.1041	3.9489	13.5559	4.8543
	99% confidence level	20.6008	11.7408	12.4229	3.9780	12.0849	4.9607
Gamma	95% confidence level	25.4870	12.0189	13.3205	4.0577	14.0315	5.0596
	99% confidence level	23.9104	13.1328	13.0372	4.2156	13.4129	5.4324
Logistic	95% confidence level	25.1926	11.8616	13.2986	4.0421	13.9539	4.9884
	99% confidence level	22.0841	12.5543	12.8603	4.1972	13.0315	5.3303
Gumbel	95% confidence level	26.6035	14.4410	4.1374	13.5354	14.4593	5.2103
	99% confidence level	26.2648	14.4655	4.4840	13.4743	14.3349	5.9853

The root-mean square errors (RMSE) obtained from the OR and LR methods are presented in Table 5. It allows to verify that the root-mean square errors (RMSE) obtained from the OR method are slightly larger than that from the LR method.

3. Castillo & Fernández-Canteli (Cfc) method

Castillo and Fernández-Canteli (CFC) [35] proposed a probabilistic Δσ-N relationship based on the Weibull distribution as expressed in Equation (11):

$$P_f(N,\Delta\sigma)=1-exp\left[-\left(\frac{(\log N-B)(\log\Delta\sigma-C)-\lambda}{\delta}\right)^{\beta}\right]V=(\log N-B)(\log\Delta\sigma-C)\geq\lambda \quad (11)$$

where: P_f is the failure probability; N is the number of cycles to failure; $\Delta\sigma$ is the stress range; B is the threshold parameter for the lifetime; C is threshold parameter for stress range, λ is threshold parameter for normalized variable V; δ is the scale parameter; β is the Shape parameter of Weibull model.

The material parameters of the CFC model are fitted based on experimental results for “SLDSR”, “DLDSR” and “SLDSR + DLDSR” test series. The fitted parameters are summarized in Table 6. The S–N curves with different probabilities are presented in Fig. 6. The results showed that the threshold parameter B and C of “SLDSR” test series is larger than that from “DLDSR” and “SLDSR + DLDSR” test series while the threshold parameter λ of the normalized variable of “SLDSR” is smaller.

4. Stochastic analysis method

In the stochastic analysis, fatigue life can be predicted by the materials parameters of S–N curves and a corresponding probability density function (PDF). This section discussed the probabilistic functions, regression methods, and exponent effects on probabilistic fatigue life.

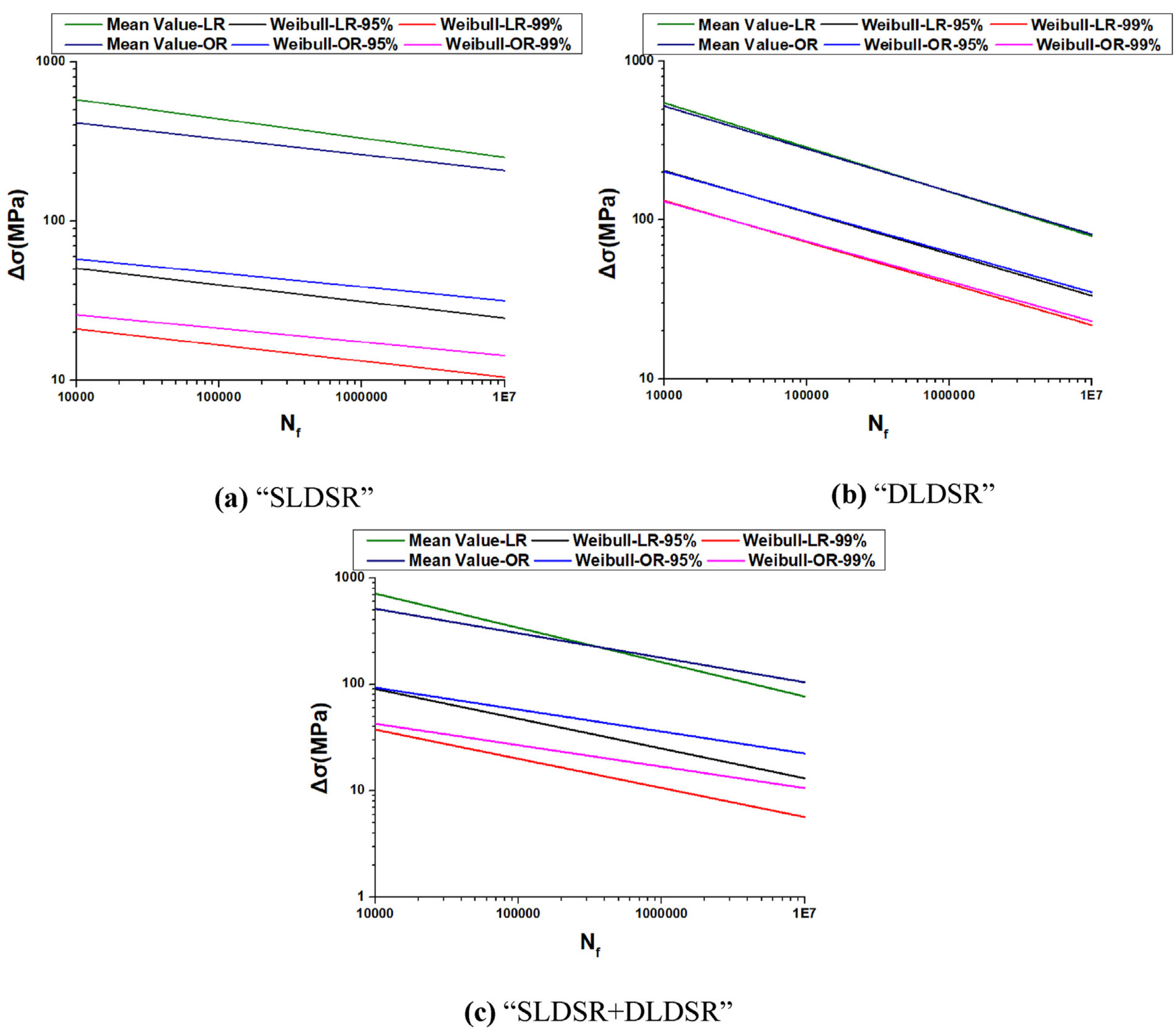

Fig. 8 – Regression method effects on probabilistic fatigue life – Weibull distribution.

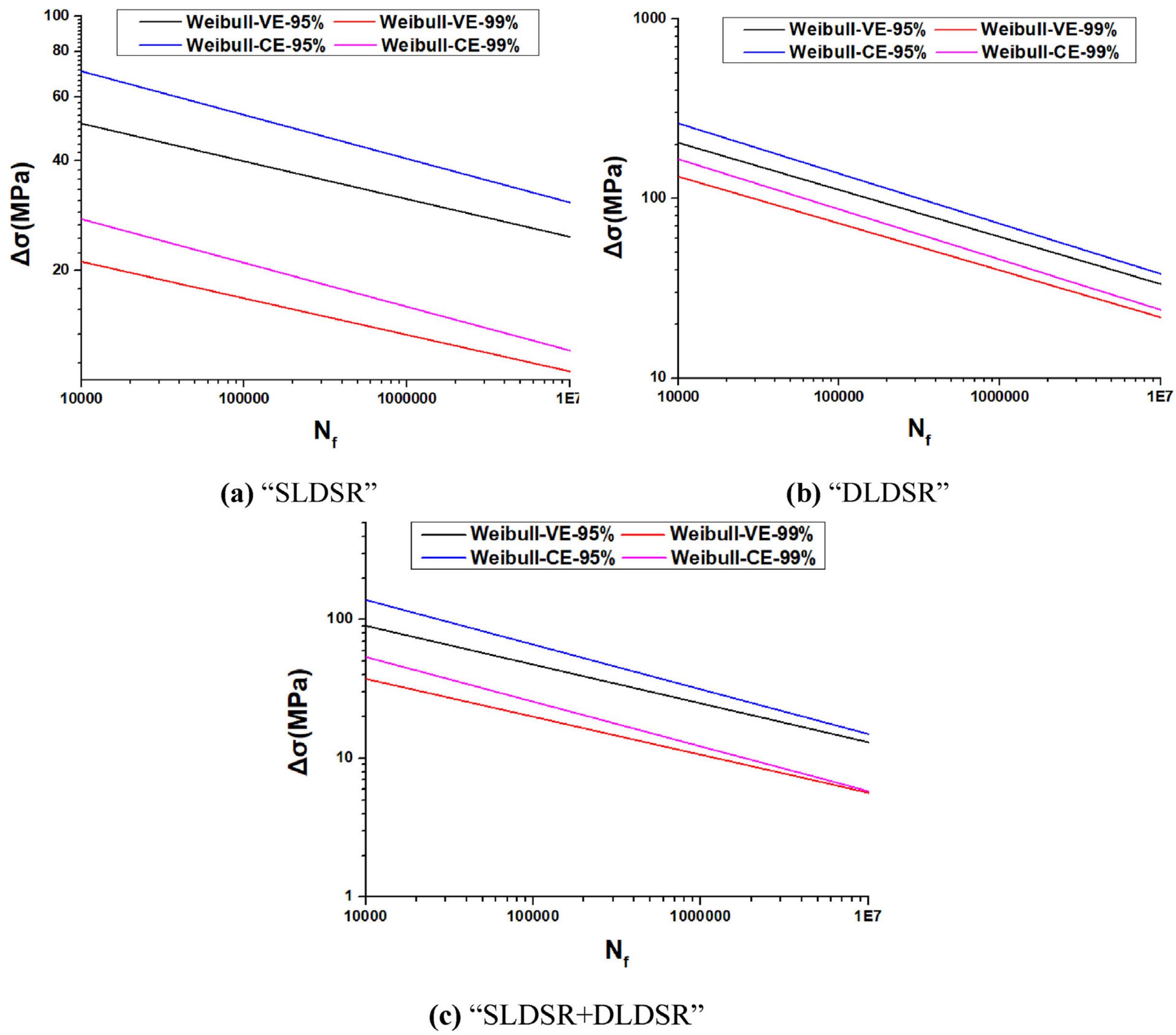

Fig. 9 – Regression method effects on probabilistic fatigue life – Weibull distribution.

4.1. *Probabilistic functions effects*

Six different probabilistic functions, namely Gaussian distribution, Lognormal distribution, Weibull distribution, Gamma distribution, Logistic distribution, and Gumbel distribution, were used to obtain the probabilistic fatigue life [42]. The Probability density function and its estimated parameters of different distributions are presented in Table 7. A stochastic analysis using Latin hypercube sampling strategies [43] of the S–N curves of the SLDSR test series using the standard derivation of the least-squares regression, for different probabilistic functions, was used. The S–N curves comparison with 95% and 99% confidence levels obtained with different probabilistic functions using the standard derivation of the least-squares regression are shown in Fig. 7. Noted that the confidence level can be calculated as one minus the failure probability in Equation (10). The results showed that the stochastic analysis with the Gumbel distribution contributed the largest fatigue strength with 95% and 99% confidence level while the stochastic analysis with the Weibull distribution led to the smallest fatigue strength with 95% and 99% confidence level. The material parameters A and B of the S–N curves with

Table 10 – The exponent effects on the probabilistic fatigue life using the standard derivation of the least-squares regression.

Functions			SLDSR		DLDSR		SLDSR + DLDSR	
			A	B	A	B	A	B
Weibull	Constant	95%	19.3562	8.3040	12.6533	3.5772	10.6457	3.1008
		99%	15.9741	8.3040	11.9397	3.5772	9.3692	3.1008
	Varied	95%	20.3990	9.6169	12.8141	3.8143	10.9911	3.5732
		99%	17.1774	9.9466	12.1291	3.8301	9.7515	3.6539

95% and 99% confidence level is fitted in terms of different test series, listed in Table 8 for the LR method and Table 9 for the OR method.

4.2. Regression method effects

The S–N curves with 95% and 99% confidence levels using different standard derivation are compared in Fig. 8a, b and c for "SLDSR", "DLDSR" and "SLDSR + DLDSR" test series for both LR and OR methods, respectively, using the Weibull distribution. The trend on the regression methods on the probabilistic fatigue life is not obvious. In terms of the "SLDSR" test series, the fatigue strength with 95% confidence level obtained using a standard derivation of LR methods is smaller than obtained using a standard derivation of LR methods, but the fatigue strength with 99% confidence level obtained using

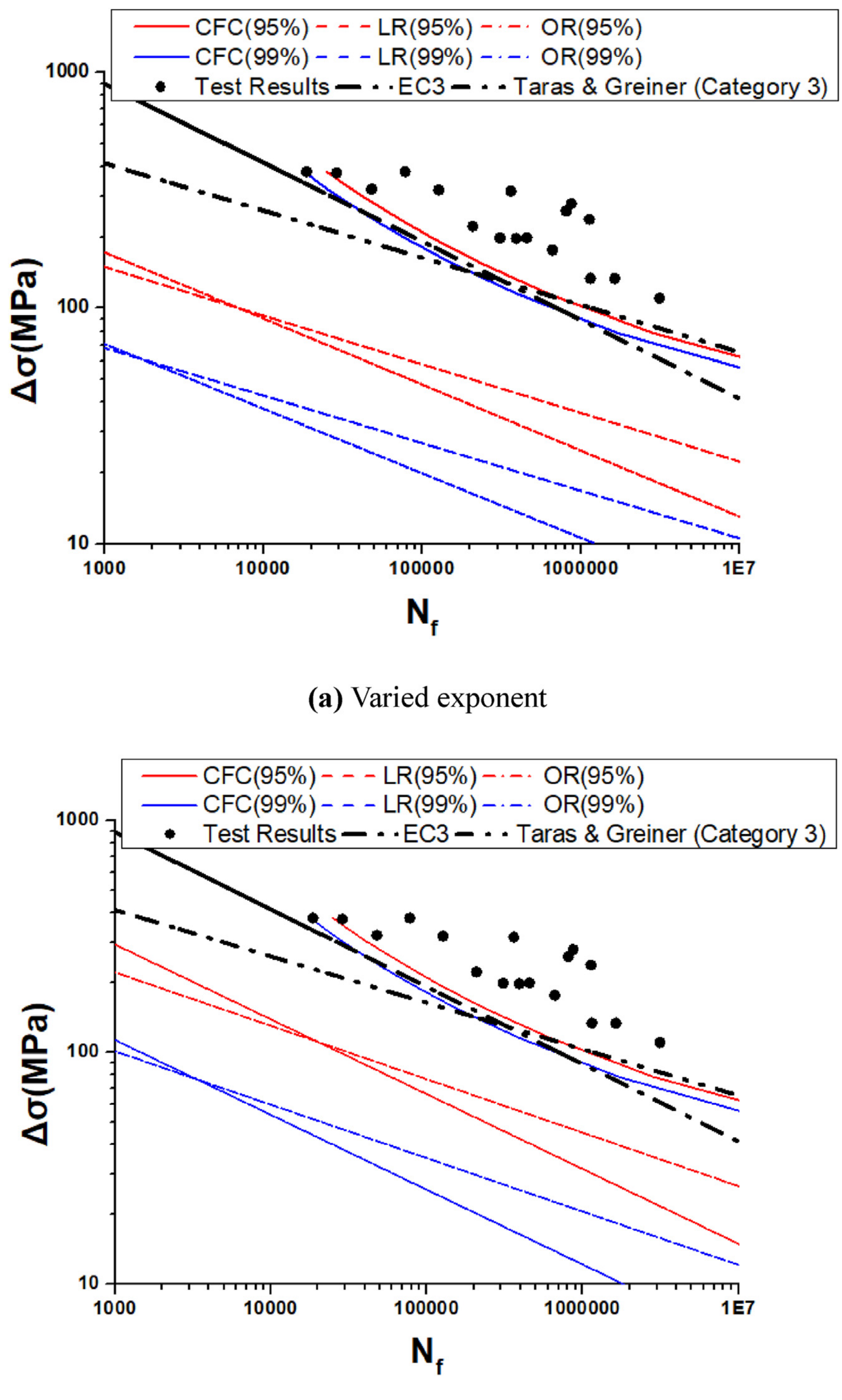

Fig. 10 – Comparison between the CFC model and stochastic analysis using the Weibull distribution.

a standard derivation of LR methods is larger than obtained using a standard derivation of LR methods. In terms of the "DLDSR" test series, the differences of the fatigue strength with 95% and 99% confidence levels obtained using a standard derivation of LR and OR methods are quite small concerning the Weibull distribution. In terms of the "SLDSR + DLDSR" test series, the fatigue strength with 95% and 99% confidence levels obtained using the LR method is smaller than the one obtained using the OR method.

4.3. *Exponent effects*

To investigate the exponent effects, the parameters B kept as a constant during stochastic analysis, denoted as "CE", while the parameters B in the previous analysis is varied with assumed probabilistic function, denoted as "VE". The S–N curves with 95% and 99% confidence levels using varied and constant exponents are compared in Fig. 9 with the lower bound using the Weibull distribution. The results showed that the fatigue strength with 95% and 99% confidence levels obtained using constant exponent is larger than using a variable parameter. The material parameters using the standard derivation of the least-squares regression with a varied and constant exponent are summarized in Table 10.

5. Comparison between Cfc and stochastic analysis method

The comparison between the test results, CFC model, stochastic analysis [43], EC3 [18] (class 71 S–N curve), and Category 3 proposed by Taras & Greiner [20,21] is shown in Fig. 10 for Weibull distribution. The results showed that the fatigue strength with both 95% and 99% confidence levels obtained using the stochastic analysis with the Weibull distribution is smaller than that of the CFC model, EC3 (class 71 S–N curve) and S–N curves of Category 3 proposed by Taras & Greiner. The probabilistic fatigue life with stochastic analysis using constant exponent is closer to the CFC model than that based on variable parameter.

6. Conclusions

With growing concern about the structural reliability and integrity, the probabilistic fatigue behaviour of riveted joints has been deserved more attention, more specifically about the influence that this may have on the fatigue damage accumulation evaluation of structural components. The fatigue life considering multiple uncertainty sources' effects is essential for the determination of the riveted details. The following conclusions could be drawn.

(1) The parameters of S–N curves for two riveted joints were obtained using the least-squares regression (LR) and the orthogonal regression (OR) methods, respectively, in this paper. The results showed that the fitted slope B from the OR method is slightly larger than that from the LR method of all specimens. In the relatively lower-stress range, the parameters from the OR method predicts the larger fatigue lives than from the LR method, detailed as $0 < \Delta\sigma \leq 305$ MPa for SLDSR specimen, $0 < \Delta\sigma \leq 160$ MPa for DLDSR specimen, and $0 < \Delta\sigma \leq 223$ MPa for "SLDSR + DLDSR" results. In the upper-stress range, the parameters from the OR method predict the smaller fatigue life than from the LR method, detailed as $\Delta\sigma > 305$ MPa for SLDSR specimen, $\Delta\sigma > 160$ MPa for DLDSR specimen, and $\Delta\sigma > 223$ MPa for "SLDSR + DLDSR" results. Therefore, in the fatigue damage accumulation assessment of structural components, the design S–N curves based on the LR or OR methods, more precisely for high-cycle regimes, may estimate substantially different damage values.

(2) The probabilistic functions, regression methods and exponent effects on the probabilistic fatigue life are discussed. Among six different probabilistic functions, the stochastic analysis with the Gumbel distribution contributed the largest fatigue strength with 95% and 99% confidence levels while the stochastic analysis with the Weibull distribution led to the smallest fatigue strength with 95% and 99% confidence levels. The effects of regression methods on probabilistic fatigue life are not obvious. The fatigue strength with 95% and 99% confidence levels obtained using constant exponent is larger than that resulting from variable exponent.

(3) The fatigue strength with both 95% and 99% confidence rate obtained using the stochastic analysis with the Weibull distribution is smaller than that provided by the CFC model, EC3 and S–N curves of Category 3 proposed by Taras & Greiner. The probabilistic fatigue life with stochastic analysis using constant exponent is closer to the CFC model than using variable exponent.

Credit authorship Contribution statement

José Correia: formal analysis, writing - original draft, validation, supervision, writing - review & editing. **António Mourão:** formal analysis, investigation, writing - original draft. **Haohui Xin:** formal analysis, investigation, writing - original draft. **Abílio De Jesus:** formal analysis, writing - review & editing, validation, supervision. **Túlio Bittencourt:** formal analysis, validation, supervision, writing - review & editing. **Rui Calçada:** formal analysis, validation, supervision, writing - review & editing. **Filippo Berto:** formal analysis, validation, writing - review & editing.

Declaration of competing interest

The authors declare that they have no known competing financial interests or personal relationships that could have appeared to influence the work reported in this paper.

Acknowledgments

This research was supported by: project grant (PTDC/ECI-EST/30103/2017) FiberBridge - Fatigue strengthening and assessment of railway metallic bridges using fiber-reinforced polymers by FEDER funds through COMPETE2020 (POCI) and by national funds (PIDDAC) through the Portuguese Science Foundation (FCT/MCTES); and, base funding - UIDB/04708/2020 and programmatic funding - UIDP/04708/2020 of the CONSTRUCT - Instituto de I&D em Estruturas e Construções - funded by national funds through the FCT/MCTES (PIDDAC). António Mourão would like to thank the Ph.D. research grant (PD/BD/150306/2019) awarded by national funds (PIDDAC) through the Portuguese Science Foundation (FCT/MCTES). The author Haohui Xin gratefully acknowledges the financial support provided by the National Natural Science Foundation (Grants #51808398 & 52078362) of the People's Republic of China. José Correia would like to thank the individual project grant (2020.03856.CEECIND) awarded by national funds (PIDDAC) through the Portuguese Science Foundation (FCT/MCTES).

REFERENCES

[1] Xin H, Nijgh M, Veljkovic M. Computational homogenization simulation on steel reinforced polymer used in the injected bolted connections. Compos Struct 2019;210:942–57.
[2] De Jesus AMP, Pinto H, Fernández-Canteli A, Castillo E, Correia JAFO. Fatigue assessment of a riveted shear splice based on a probabilistic model. Int J Fatig 2010;32:453–62.
[3] Xin H, Veljkovic M. Residual stress effects on fatigue crack growth rate of mild steel S355 exposed to air and seawater environments. Mater Des 2020:108732.
[4] Xin H, Correia JAFO, Veljković M. Three-dimensional fatigue crack propagation simulation using extended finite element methods for steel grades S355 and S690 considering mean stress effects. Engineering structures. Eng Struct 2020;227:111414.
[5] Mohammad AE. Fatigue in riveted railway bridges". PhD Thesis. Chalmers University of Technology; 2002.
[6] Crocetti R. On some fatigue problems related to steel bridges. Chalmers University of Technology; 2001.
[7] Åkesson B. Fatigue life of riveted railway bridges". PhD Thesis. Chalmers University of Technology; 1994.
[8] Barbosa JF, Correia JAFO, Montenegro P, Júnior RCSF, Lesiuk G, De Jesus AMP, et al. A comparison between SN Logistic and Kohout-Věchet formulations applied to the fatigue data of old metallic bridges materials. Frat Ed Integrità Strutt 2019;13:400–10.
[9] Pipinato A, Molinari M, Pellegrino C, Bursi OS, Modena C. Fatigue tests on riveted steel elements taken from a railway bridge. Struct Infrastruct Eng 2011;7:907–20.
[10] Leonetti D, Maljaars J, Snijder HHB. Fitting fatigue test data with a novel SN curve using frequentist and Bayesian inference. Int J Fatig 2017;105:128–43.
[11] Pedrosa B, Rebelo C, Gervásio H, da Silva LS, Correia JA. Fatigue of preloaded bolted connections with injection bolts. Struct Eng Int 2020;30:102–8.
[12] Imam BM, Righiniotis TD. Fatigue evaluation of riveted railway bridges through global and local analysis. J Constr Steel Res 2010;66:1411–21.
[13] Al-Emrani M. Fatigue in Riveted Railway Bridges-a study of the fatigue performance of riveted stringers and stringer-to-floor-beam connections. Chalmers University of Technology; 2002.
[14] Al-Emrani M. Fatigue performance of stringer-to-floor-beam connections in riveted railway bridges. J Bridge Eng 2005;10:179–85.
[15] Toasa Caiza PD, Ummenhofer T, Correia JAFO, De Jesus A. Applying the Weibull and Stüssi methods that derive reliable Wöhler curves to historical German bridges. Pract Period Struct Des Construct 2020;25:4020029.
[16] Pedrosa B, Correia JAFO, Rebelo C, Lesiuk G, De Jesus AMP, Fernandes AA, et al. Fatigue resistance curves for single and double shear riveted joints from old Portuguese metallic bridges. Eng Fail Anal 2019;96:255–73.
[17] da Silva ALL, Correia JAFO, de Jesus AMP, Figueiredo MAV, Pedrosa BAS, Fernandes AA, et al. Fatigue characterization of a beam-to-column riveted joint. Eng Fail Anal 2019;103:95–123.
[18] European Committee for Standardization (CEN). EN 1993-1-9: Eurocode 3:Design of steel structures, part 1–9: fatigue. Brussels: European standard; 2004.
[19] Kühn B, Lukic M, Nussbaumer A, Günther H-P, Helmerich R, Herion S, et al. Assessment of existing steel structures: recommendations for estimation of remaining fatigue life. Joint Research Center; 2008.
[20] Taras A, Greiner R. Statistical background to the proposed fatigue class catalogue for riveted components. Report: contribution to WG6. 1—assessment of existing steel structures. ECCS TC6—2010, spring Meet.; 2010.
[21] Taras A, Greiner R. Development and application of a fatigue class catalogue for riveted bridge components. Struct Eng Int 2010;20:91–103.
[22] Pedrosa B, Correia JAFO, Rebelo CAS, Veljkovic M. Reliability of fatigue strength curves for riveted connections using normal and Weibull distribution functions. ASCE-ASME J Risk Uncertain Eng Syst Part A Civ Eng 2020;6:4020034.
[23] de Jesus AMP, da Silva ALL, Correia JAFO. Fatigue of riveted and bolted joints made of puddle iron—an experimental approach. J Constr Steel Res 2015;104:81–90.
[24] Leite RCG, de Jesus AMP, Correia J, Raposo P, Jorge RN, Parente MP, et al. A methodology for a global-local fatigue analysis of ancient riveted metallic bridges. Int J Struct Integr 2018;9(3):355–80.
[25] Mayorga LG, Sire S, Correia JAFO, De Jesus AMP, Rebelo C, Fernández-Canteli A, et al. Statistical evaluation of fatigue strength of double shear riveted connections and crack growth rates of materials from old bridges. Eng Fract Mech 2017;185:241–57.
[26] Correia JAFO, Correia M, Holm M, Ekeborg J, Lesiuk G, Castro JM, et al. Evaluation of fatigue design curves for a double-side welded connection used in offshore applications. Press Vessel Pip Conf 2018;51678:V06AT06A028. American Society of Mechanical Engineers.
[27] Correia J, De Jesus AMP, Silva ALL, Pedrosa B, Rebelo C, Calçada R. FE simulation of SN curves for a riveted connection using two-stage fatigue models. Adv Comput Des an Int J 2017;2:333–48.
[28] Sire S, Ragueneau M. Fatigue design of metallic railway bridges in France at the end of the nineteenth century. Proc Inst Civ Eng Eng 2020;1–8.
[29] Sire S, Toasa Caiza PD, Espion B, Ragueneau M. Contribution to the study of the influence of the stress ratio on the high cycle fatigue behaviour of riveted joints. Fatig Fract Eng Mater Struct 2020;43(12):3027–36.
[30] Fisher JW, Yen BT, Wang D. Fatigue strength of riveted bridge members. J Struct Eng 1990;116:2968–81.
[31] Maljaars J, Leonetti D, Maas C. Fatigue life prediction of hot riveted double covered butt joints. Int J Fatig 2019;124:99–112.

[32] Leonetti D, Maljaars J, Snijder HHB. Fatigue life prediction of hot-riveted shear connections using system reliability. Eng Struct 2019;186:471–83.
[33] Raposo P, Correia JAF de O, De Jesus AMP, Calçada RAB, Lesiuk G, Hebdon M, et al. Probabilistic fatigue SN curves derivation for notched components. Frat Ed Integrità Strutt 2017;11.
[34] Correia JAFO, De Jesus AMP, Fernández-Canteli A. Local unified probabilistic model for fatigue crack initiation and propagation: application to a notched geometry. Eng Struct 2013;52:394–407.
[35] Castillo E, Fernandez-Canteli A. A unified statistical methodology for modeling fatigue damage. Springer Science & Business Media; 2009.
[36] Zhu S-P, He J-C, Liao D, Wang Q, Liu Y. The effect of notch size on critical distance and fatigue life predictions. Mater Des 2020:109095.
[37] Zhu S-P, Huang H-Z, Peng W, Wang H-K, Mahadevan S. Probabilistic physics of failure-based framework for fatigue life prediction of aircraft gas turbine discs under uncertainty. Reliab Eng Syst Saf 2016;146:1–12.
[38] Silva ALL, Correia José AFO, Xin Haohui, Lesiuk Grzegorz, De Jesus Abílio MP, Fernandes Fb AA. Fatigue strength assessment of riveted details in railway metallic bridges. Eng Fail Anal 2020. https://doi.org/10.1016/j.engfailanal.2020.105120.
[39] Basquin OH. The exponential law of endurance tests. Proc Am Soc Test Mater 1910;10:625–30.
[40] Björck Å. Numerical methods for least squares problems. SIAM; 1996.
[41] Carroll RJ, Ruppert D. The use and misuse of orthogonal regression in linear errors-in-variables models. Am Statistician 1996;50:1–6.
[42] Barbosa JF, Correia JAFO, Freire Júnior RCS, Zhu S-, De Jesus AMP. Probabilistic S-N fields based on statistical distributions applied to metallic and composite materials: state of the art. Adv Mech Eng 2019;11(8):1–22.
[43] Lataniotis C, Marelli S, Sudret B. UQLab user manual—The Input module. Chair risk, Saf Uncertain Quantif ETH Zurich, vols. 2–102. Zurich, Switzerland: Rep No UQLab-V1; 2015.